# Connectome dysfunction in patients at clinical high risk for psychosis and modulation by oxytocin

**Running title:** Connectome dysfunction & oxytocin in psychosis risk

**Authors**

Cathy Davies[*1,2,3], Daniel Martins[*3,4], Ottavia Dipasquale[3], Robert A. McCutcheon[2,5], Andrea De Micheli[1,4], Valentina Ramella-Cravaro[1], Umberto Provenzani[1,6], Grazia Rutigliano[1], Marco Cappucciati[1], Dominic Oliver[1,5], Steve Williams[3], Fernando Zelaya[3], Paul Allen[2,7,8], Silvia Murguia[9], David Taylor[10], Sukhi Shergill[2], Paul Morrison[2], Philip McGuire[5,11,12], Yannis Paloyelis[†3], Paolo Fusar-Poli[†1,4,6,13]

**Affiliations**

1. Early Psychosis: Interventions & Clinical-detection (EPIC) Lab, Department of Psychosis Studies, Institute of Psychiatry, Psychology & Neuroscience, King's College London, London, UK;
2. Department of Psychosis Studies, Institute of Psychiatry, Psychology & Neuroscience, King's College London, London, UK;
3. Department of Neuroimaging, Institute of Psychiatry, Psychology & Neuroscience, King's College London, London, UK;
4. National Institute for Health Research (NIHR) Biomedical Research Centre (BRC), South London and Maudsley NHS Foundation Trust, London, UK;
5. Department of Psychiatry, University of Oxford, Oxford, UK;
6. Department of Brain and Behavioral Sciences, University of Pavia, Pavia, Italy;
7. Department of Psychology, University of Roehampton, London, UK;
8. Icahn School of Medicine, Mount Sinai Hospital, New York, NY, USA;
9. Tower Hamlets Early Detection Service, East London NHS Foundation Trust, London, UK;
10. Institute of Pharmaceutical Science, King's College London, London, UK;
11. NIHR Oxford Health Biomedical Research Centre, Oxford, UK;
12. Oxford Health NHS Foundation Trust, Oxford, UK;
13. Outreach And Support in South London (OASIS) Service, South London and Maudsley NHS Foundation Trust, London, UK.

* These authors contributed equally to this work. † These authors share senior authorship.

**Corresponding author:** Dr Cathy Davies, Department of Neuroimaging, Institute of Psychiatry, Psychology & Neuroscience, King's College London, DeCrespigny Park, London, UK, SE5 8AF. Email: cathy.davies@kcl.ac.uk



**Word count:** Abstract = 260 | Text = 4,890 | Tables: 2 | Figures: 3 | Refs: 100

## ABSTRACT

Abnormalities in functional brain networks (functional connectome) are increasingly implicated in people at Clinical High Risk for Psychosis (CHR-P). Intranasal oxytocin, a potential novel treatment for the CHR-P state, modulates network topology in healthy individuals. However, its connectomic effects in people at CHR-P remain unknown. Forty-seven men (30 CHR-P and 17 healthy controls) received acute challenges of both intranasal oxytocin 40 IU and placebo in two parallel randomised, double-blind, placebo-controlled cross-over studies. Multi-echo resting-state fMRI data was acquired at approximately 1h post-dosing. Using a graph theoretical approach, the effects of group (CHR-P vs healthy control), treatment (oxytocin vs placebo) and respective interactions were tested on graph metrics describing the topology of the functional connectome. Group effects were observed in 12 regions (all $p_{FDR}<.05$) most localised to the frontoparietal network. Treatment effects were found in 7 regions (all $p_{FDR}<.05$) predominantly within the ventral attention network. Our major finding was that many effects of oxytocin on network topology differ across CHR-P and healthy individuals, with significant interaction effects observed in numerous subcortical regions strongly implicated in psychosis onset, such as the thalamus, pallidum and nucleus accumbens, and cortical regions which localised primarily to the default mode network (12 regions, all $p_{FDR}<.05$). Our findings provide new insights on aberrant functional brain network organisation associated with psychosis risk and demonstrate, for the first time, that oxytocin modulates network topology in brain regions implicated in the pathophysiology of psychosis in a clinical status (CHR-P vs healthy control) specific manner. Further profiling of the connectomic, clinical and cognitive effects of oxytocin in this population is warranted.

**Keywords:** graph theory, resting state, functional connectivity, psychosis risk, oxytocin, networks

## INTRODUCTION

Abnormal functional connectivity is one of the strongest biological markers associated with psychosis (1–3). Alterations in the brain's functional network organisation (functional connectome) are also observed prior to the onset of psychosis in people at Clinical High Risk (CHR-P) (4–6). These help-seeking individuals present with attenuated psychotic symptoms, emotional, cognitive and functional impairments and have a 20% two-year risk of transitioning to frank psychosis (7,8). There are currently no licensed pharmacological treatments for CHR-P patients (9,10), which represents a significant unmet clinical need. A deeper understanding of the connectomic abnormalities contributing to psychosis risk, and the potential ameliorative effects of experimental therapeutics, is urgently required.

Accumulating evidence from different imaging modalities has revealed brain-wide as well as regional dysfunction in people at CHR-P (11–13) and those with established psychosis (for reviews see (14,15)), particularly in the hippocampus, striatum, thalamus and frontal cortex—core components of the most influential circuit models of psychosis pathophysiology (16–18). Evidence of aberrant resting-state functional connectivity between brain regions (19–21) subsequently highlighted that psychosis-related dysfunction cannot entirely be described by spatially discrete differences in neural activation. Psychosis-related dysconnectivity can be identified both within and between large-scale networks, particularly involving frontoparietal, default mode and salience networks (22–24). This suggests that network-based approaches are needed to fully capture the complete spectrum of brain dysfunction associated with psychosis.

More recently, the application of graph theory (25) to neuroimaging data opened up new possibilities for exploring aberrant functional brain network organisation from micro-to-macro-scale levels of analysis (26). Using graph theory, brain regions are represented by nodes, the functional connections between nodes represented by edges, and modules defined as communities of highly intra-connected nodes that have fewer inter-module connections (27). Like any complex network, the topology (organisational properties) of the human brain shapes its capacity for information transfer, influencing higher-order functions such as cognition as well as its vulnerability to insult (26,28,29). A disruption to the finely-tuned balance of integration vs segregation may lead to loss of high-fidelity information transfer, cognitive dysfunction and the psychotic phenomenology characteristic of the CHR-P state and frank psychosis (1,27,30). Supporting this hypothesis, evidence suggests that people with established psychosis have abnormalities across global and local (node- or module-level) topological properties (27), including reduced small-worldness (31), clustering (32), hubness

(33) and modularity (34), as well as changes in global and local efficiency (2). However, the network dysfunction that precedes psychosis onset in the CHR-P state is less well characterised.

The few studies conducted to date have shown that abnormal modular organisation in CHR-P individuals at baseline is associated with a three-fold transition rate to frank psychosis (4). Further work demonstrates that CHR-P individuals who go on to transition (vs controls and non-transitions) have altered topological centrality in frontal and anterior cingulate regions (5), reduced global efficiency and clustering (6) (although global differences are not always found in this population (5,35)), regional changes in nodal efficiency correlating with symptom severity (6), and extensive reorganisations of network community structure across most of the large-scale resting-state networks (6). Together, these data suggest that further mapping of CHR-associated functional connectomic alterations—and how they respond to experimental therapeutics—would not only enrich understanding of the neurobiological mechanisms driving psychosis onset but may also illuminate novel treatment targets.

One potential novel treatment is the neuropeptide oxytocin, which has neurobehavioural effects in multiple domains that could be beneficial for CHR-P individuals. These include anxiolytic effects (36), modulation of social and emotional cognition (37–40), hypothalamic-pituitary-adrenal axis regulation (36) and parasympathetic modulation of the heart rhythm (41). In our previous CHR-P work, we demonstrated that oxytocin modulates frontal activation during mentalising (42), anterior cingulate neurochemistry (43) and resting cerebral blood flow in the hippocampus among numerous other regions (44). Independent evidence further suggests that oxytocin modulates connectivity within resting-state networks in healthy volunteers (45,46) and ‘normalises’ aberrant connectivity in several clinical populations, including patients with social anxiety (47), post-traumatic stress disorder (48) and autism (49). Moreover, a recent study in healthy males demonstrated that a single dose of oxytocin was sufficient to modulate local functional network topology, including in regions and networks implicated in the pathophysiology of psychosis (50). This raises the possibility that oxytocin may ameliorate the connectomic dysfunction present in CHR-P individuals. It is unclear, however, whether oxytocin will have similar connectomic effects in CHR-P patients as in healthy controls. Supporting the hypothesis that a differential effect may exist is our recent finding that oxytocin increases cardio-parasympathetic activity in CHR-P but not in healthy males (41).

To address this gap, in this study we took a data-driven approach combining multi-echo resting-state blood-oxygen-level-dependent (BOLD) functional magnetic resonance imaging

(fMRI) with graph-theory modelling. We investigated differences in global and regional topology of the functional connectome related to (a) CHR-P status (CHR-P patients vs controls; group effects), (b) the main effects of intranasal oxytocin vs placebo (treatment effects), and (c) group x treatment interactions to identify clinical status-specific effects of oxytocin.

## SUBJECTS & METHODS

### Participants

Thirty male, help-seeking CHR-P individuals aged 18-35 were recruited from a specialist early detection service in London, UK (51). A CHR-P status was determined using the Comprehensive Assessment of At-Risk Mental States (CAARMS) 12/2006 criteria (52). Seventeen healthy male controls, aged 19-34, were recruited as part of a related study (see below) (50). Full inclusion and exclusion criteria are detailed in the Supplementary Methods. In both studies, subjects were asked to abstain from using recreational drugs for at least 1 week and alcohol for at least 24 hours prior to each session. Urine screening was conducted before each session. The study received Research Ethics approval (London Bridge Committee: 14/LO/1692 and King's College London Committee: PNM/13/14-163) and all subjects gave written informed consent.

### Design, Materials, Procedure

CHR-P and control data were combined from two related studies which were collaboratively designed so that their data could be analysed together. The CHR-P study (ISRCTN48799530) used a randomised, double-blind, single-dose challenge of intranasal oxytocin versus placebo in a crossover design (one-week wash-out). Participants self-administered 40 IU intranasal oxytocin or placebo using a standard nasal spray, as per our in-house protocol following recommended guidelines (Supplementary Materials) (53). Participants were randomly allocated to a treatment order (oxytocin/placebo or placebo/oxytocin). Following drug administration, participants underwent a battery of MRI sequences which started in the morning period to minimise potential effects of diurnal variation in oxytocin or vasopressin (54). Healthy control data came from a related randomised, double-blind, single-dose triple-dummy crossover study (50), where participants received oxytocin/placebo via three administration routes (nasal spray, nebulizer and intravenous infusion) in one of two fixed sequences: either nebulizer/intravenous/spray, or spray/intravenous/nebulizer. In three out of four sessions only one route of administration contained the active drug; in the fourth session, all routes delivered placebo or saline. The dose administered intranasally was 40 IU. For this study, we only used data from the placebo and nasal spray arms to maximise comparability to the protocol used in the CHR-P sample. Therefore, dose, device for drug administration, scanner and time post-dosing were matched across studies.

### MRI Acquisition, Preprocessing and Denoising

All scans were conducted on a General Electric Discovery MR750 3 Tesla system (General Electric, Chicago, USA) using a 32-channel head coil. The 8 min 10 s multi-echo resting-state

fMRI scan was obtained starting at (M±SD) 62.6±3.1 min post-dosing in the CHR-P group and 57.01±3.38 min in healthy controls. Acquisition parameters, image preprocessing and denoising procedures (performed using the AFNI (55) tool meica.py (56,57)) are detailed in the Supplementary Methods.

**Functional Connectivity**

Figure 1 provides an overview of the network analysis steps. To generate brain-wide functional connectivity matrices for each subject and treatment condition, we first extracted the BOLD time courses for each of the 66 cortical anatomical regions-of-interest (ROIs) included in the Desikan-Killiany atlas (58), with the addition of 9 bilateral subcortical regions (cerebellum, thalamus, caudate, putamen, pallidum, hippocampus, amygdala, accumbens, ventral diencephalon) and brainstem from the Harvard-Oxford Atlas, for each participant/session using *fslmeants* from the FMRIB Software Library (FSL). The bilateral frontal pole had poor coverage in our data and thus these 2 nodes were removed, leaving 83 nodes. We generated bivariate Pearson's correlation matrices for the time courses of all possible pairs of ROIs (83x83) using Matlab/R2015b. Finally, we normalised our correlation measures to z-scores using the Fisher r-z transform. To ensure that any graph metric results were not driven by patient-control differences in overall connectivity strength (59), we examined mean functional connectivity, calculated as the average of the elements in the lower triangular matrix for each subject/condition.

**Graph Estimation and Network Characterisation**

Our z-transformed connectivity matrices were then used to construct brain graphs representing the functional connectome for each subject/condition, using an undirected signed weighted approach (28). From the fully weighted networks we calculated equi-sparse networks by retaining a fixed percentage (K) of the total amount of possible edges. In order to determine systematic differences in the network's topological organisation that are not dependent on the choice of an arbitrary threshold, we chose a range of sparsity thresholds from 5 to 34%, with steps of 1%, based on previous evidence showing the characteristic small-world behaviour of human brain networks is most consistently observed for this range (60). For each brain network and sparsity level, we used the Matlab functions provided with the Brain Connectivity Toolbox (28) to compute one global (global efficiency) and three nodal network metrics: betweenness-centrality, local efficiency and node degree. Details on the calculation of each of these metrics have been described elsewhere (28) but a brief overview is provided in Supplementary Figure S1. For each of the graph metrics analysed, we summarised the different values over the range of thresholds using the area under the curve

(AUC), providing a summary estimator for each graph metric that is independent of single threshold selection and which is sensitive to topological differences in brain networks (61,62). All of our statistical analyses on graph metrics were therefore run on AUC parameters rather than the raw values.

**<Figure 1>**

**Statistical Analysis**

We investigated group differences, treatment effects and (group x treatment) interactions across micro-to-macro-scale levels of functional connectome organisation. Specifically, we examined mean connectivity strength and global efficiency of the whole-brain network, the three nodal graph metrics, and individual connections between pairs of nodes. To evaluate the main effect of group (i.e. differences related to CHR-P status), treatment conditions were collapsed by calculating a mean average per subject and 2-sample t-tests conducted. For the main effect of treatment, oxytocin minus placebo (difference) values were calculated per subject and one-sample t-tests conducted. To examine interactions, the difference values were entered into two-sample (CHR-P vs control) t-tests. These analyses were conducted in Matlab and the directionality of significant interactions was determined by examining subject-level values.

***Global Metrics.*** We calculated mean connectivity strength and global efficiency of the brain network for each participant and treatment condition and compared groups, treatments and interactions using the relevant t-tests, as above. Group differences in mean connectivity during the placebo condition (only) were also examined with a 2-sample t-test.

***Node Level Metrics.*** We retrieved values for the betweenness-centrality, local efficiency and degree of each node of the connectome for each subject and treatment condition. Average and difference values were computed (as above) to examine the main effects of group, treatment and interaction effects using t-tests (as above), controlling false positives with FDR correction for the number of nodes examined.

***Edge Level Metrics***. To investigate differences in each individual edge of the connectivity matrices, we used the Network Based Statistics (NBS) method (63) implemented in the NBS toolbox v1.2 to control the family-wise error rate (in the weak sense) when mass-univariate testing is performed at every edge of the graph. While this approach does not allow for inferences on individual connections, it allows extraction of subnetworks or topological clusters of regions that are significantly differently connected between groups and conditions (63).

When compared to analyses at the individual edge level, the NBS method offers greater sensitivity while also controlling for false positives (63). In our NBS analysis, we tested for effects of group, treatment and interactions each using three arbitrary primary thresholds: 1.5, 3.1 and 4. We then used a two-tailed significance threshold of $p<.05$, with 5000 permutations.

For all analyses, statistical significance was set at $p<.05$ after correction for multiple testing, when applicable. Results were visualised using ENIGMA toolbox v2 (64), MRIcron and BrainNet Viewer. In the main text visualisation, all significant results were presented together on one brain template irrespective of the metric (betweenness-centrality, node degree and local efficiency), by assigning all significant t-statistics to their respective regions across metrics. Where there were effects in the same region in more than one metric, the larger t-value was shown. Further supplementary visualisations depicted results by individual metrics.

**Overlap with Large-Scale Resting-State Networks**

To maximise the interpretability of our findings and facilitate comparisons with previous work focusing on large-scale resting-state networks (RSNs) (45,50), we quantified the percentage of overlap (Dice-kappa coefficient) between our group, treatment and interaction effect maps (separately) and each of the RSNs described in the atlas from Yeo et al (65), as detailed in the Supplementary Material and Fig 3. These values provide a qualitative contextualisation of our main findings which the reader can use for quick comparisons with previous literature.

## RESULTS

### Sample Characteristics

Demographic and clinical characteristics of the sample are presented in Table 1. There were significantly more smokers in the CHR-P relative to the control group. One CHR-P subject was removed due to protocol violations and another omitted due to excessive head movement, leaving a sample of 28 CHR-P individuals and 17 controls.

**<Table 1>**

### Main Effect of Group (CHR-P vs Healthy Controls)

*Global metrics:* There was no main effect of group ($t(43) = -0.86$, $p = .39$), nor any difference between groups when comparing the placebo conditions alone ($t(43) = -0.82$, $p = .42$) on mean functional connectivity. There were no significant group effects ($t(43) = -1.59$, $p = .12$) on global efficiency.

*Betweenness-centrality:* Across conditions (oxytocin and placebo conditions combined), compared to healthy controls, CHR-P individuals had lower betweenness-centrality of the left caudal middle frontal gyrus and left insula, but greater betweenness-centrality of the right inferior and superior temporal gyri.

*Nodal degree:* CHR-P individuals had lower node degree of the left lingual gyrus compared to controls, but greater node degree of the right lateral orbitofrontal cortex and right pars triangularis.

*Local efficiency:* Compared to controls, CHR-P individuals had greater local efficiency of the bilateral pericalcarine cortex, bilateral rostral middle frontal gyrus and right pars orbitalis. There were no regions where local efficiency was significantly greater in controls vs the CHR-P group.

Details of significant nodal metric results are presented in Table 2 and Fig 2, with metric-level figures appended in Fig S2.

*Subnetworks:* The NBS analyses did not identify any subnetworks where there were significant effects of group on connectivity after correcting for multiple testing, irrespective of the primary threshold used.

*Overlap with RSNs:* The pathways for which we identified significant nodal differences between CHR-P individuals and controls overlapped primarily with regions belonging to the frontoparietal network (Dice coefficient = 0.58) and to a lesser extent, the limbic network (Dice coefficient = 0.26). The overlap with other networks was numerically weaker. All overlap findings are displayed in Fig 3.

**<Figure 2>**

**Main Effect of Treatment (Oxytocin vs Placebo)**

*Global metrics:* There were no significant treatment effects on mean functional connectivity ($t(44) = 1.27$, $p = .21$) nor global efficiency ($t(44) = 0.44$, $p = .66$).

*Betweenness-centrality:* Over all individuals (CHR-P and controls combined), compared to placebo, oxytocin increased the betweenness-centrality of the brainstem, while it decreased the betweenness-centrality of the left supramarginal gyrus and right insula.

*Nodal degree:* Compared to placebo, oxytocin increased node degree of the left precentral gyrus. There were no regions where oxytocin decreased node degree.

*Local efficiency:* Compared to placebo, oxytocin increased the local efficiency of the bilateral paracentral lobule and the right pars opercularis. There were no regions where oxytocin decreased local efficiency.

Details of significant nodal results are presented in Table 2, Fig 2 and Fig S3.

*Subnetworks:* The NBS analyses did not identify any subnetworks where there were significant treatment effects on connectivity after correcting for multiple testing, irrespective of the primary threshold used.

*Overlap with RSNs*: The pathways for which we identified significant nodal modulatory effects of oxytocin overlapped primarily with regions belonging to the ventral attention (Dice coefficient = 0.48) and somatomotor (Dice coefficient = 0.31) networks (Fig 3).

**Interaction Effects (Group x Treatment)**

*Global metrics:* There were no significant interaction effects on mean functional connectivity ($t(43) = -0.25$, $p = .80$) nor global efficiency ($t(43) = -0.85$, $p = .40$).

*Betweenness-centrality:* Significant interaction effects were observed in a number of brain regions. In CHR-P individuals, compared to placebo, oxytocin increased the betweenness-centrality of the left thalamus, right pallidum and right precentral gyrus, whereas in controls, the betweenness-centrality in these regions was decreased after oxytocin. Conversely, in the left nucleus accumbens, left precuneus and left superior frontal gyrus, compared to placebo, oxytocin decreased betweenness-centrality in CHR-P individuals whereas it increased betweenness-centrality in controls.

*Nodal degree:* Two regions showed significant interaction effects. In CHR-P individuals, relative to placebo, oxytocin decreased node degree of the left precuneus cortex and left superior frontal gyrus, while node degree of these regions increased in controls after oxytocin vs placebo.

*Local efficiency:* Significant interaction effects were observed for four nodes. In CHR-P individuals, compared to placebo, oxytocin increased the local efficiency of the bilateral entorhinal cortex and right temporal pole. In each of these, oxytocin decreased the local efficiency in controls. The opposite pattern was observed in the left pericalcarine cortex, with oxytocin (vs placebo) decreasing the local efficiency in CHR-P individuals but increasing it in controls.

Details of significant nodal results are presented in Table 2, Fig 2 and Fig S4.

*Subnetworks:* The NBS analyses did not identify any subnetworks where there were significant interaction effects on connectivity after correcting for multiple testing, irrespective of the primary threshold used.

*Overlap with RSNs*: The pathways for which we identified significant nodal interaction effects overlapped primarily with regions belonging to the default-mode network (Dice coefficient = 0.35; Fig 3).

**<Table 2>**

**<Figure 3>**

## DISCUSSION

Using a data-driven approach, we investigated differences in the topology of the functional connectome—at multiple levels of its hierarchical organisation—in people at CHR-P and examined whether intranasal oxytocin might attenuate some of these differences. We first demonstrated that (a) CHR-P individuals exhibit predominantly greater local graph metrics compared to healthy controls in regions most localised to the frontoparietal network, while normative global network efficiency is preserved, and (b) that oxytocin mainly produced increases in local graph metrics, predominantly in the ventral attention network. The major—and novel—finding of the current study was that many effects of oxytocin on network topology differ across CHR-P and healthy individuals, with significant interaction effects observed in numerous brain regions strongly implicated in psychosis onset, which localised primarily to the default mode network. Collectively, these findings provide new insights on alterations in functional network organisation associated with psychosis risk. Furthermore, they provide the first *in vivo* evidence that oxytocin modulates network topology in regions implicated in the pathophysiology of psychosis in a clinical status (CHR-P vs healthy control) specific manner, which strengthens the rationale for future studies investigating the therapeutic role of oxytocin in this clinical population.

### Differences in Network Topology Related to CHR-P Status

Our first finding was that most differences in local network topology related to CHR-P status (i.e. group effects) reflected greater nodal centrality in patients compared to controls. These effects mapped primarily to the frontoparietal resting state network, a major cognitive control system shown to be impaired in patients across the psychosis continuum (66,67) and transdiagnostic pathological conditions (68–70). Notably, we found greater local efficiency and nodal degree in CHR-P individuals across numerous frontal regions, indexing greater integration and importance of these nodes in the network, respectively (28). Despite the relatively few studies to have examined graph metrics in CHR-P cohorts to date, our results are supported by previous findings of increased toplogical centrality (5) and/or altered modular assignment (4,6) of these regions in CHR-P and established psychosis (33) samples.

Importantly, our group effects emerged against a backdrop of no differences in raw connectivity strength, suggesting that these nodal differences are instead signatures of a reorganisation of the brain's functional network architecture (4,27). Whether these changes arise through proximal frontal dysfunction, or reflect compensatory changes in response to dysfunctional network dynamics occurring elsewhere (27), is unclear. Conceptually, however, such reorganisations of network architecture are thought to lead to inefficient information flow,

aberrant input integration and manifestation of the psychotic and cognitive symptoms (1,27,30) characteristic of the CHR-P state, the latter of which may be particularly relevant given that half of our group differences were localised to the frontal cortex. Conversely, the lack of differences we observed in global efficiency suggests that *global* capacity for information transfer is preserved in our CHR-P sample. This is consistent with some (5) (but not all (6)) previous literature, including a large multi-cohort study using age-matched controls across the psychosis spectrum (35). Together, these findings lend support to the idea that the connectomic dysfunction preceding psychosis onset may be more subtle and characterised by changes in local functional network architecture (35).

**Effects of Oxytocin on Network Topology**

We next showed that across all measures of local network topology, oxytocin predominantly increased graph metrics compared to placebo. Of particular interest was the finding that oxytocin increased betweenness-centrality in the brainstem. High betweenness-centrality reflects nodes that participate in a large number of shortest paths in the network, thereby acting as 'bridging nodes' that mediate information flow and network integration (28,71). Our findings accord with those in a previous overlapping study in healthy controls, where oxytocin increased the nodal degree—an index of the importance of a node, equal to its number of edges—also in the brainstem (50). The brainstem is considered a key autonomic hub in models of dopamino-oxytocinergic-mediated social and emotional cognition (72), is a purported substrate for salience detection (73) (through connections with the ventral tegmental area [VTA] and mesolimbic dopamine pathway (74)) and is one potential mediator of the tuning effects of oxytocin on these processes (73). Consistent with this, we found that oxytocin-induced changes in graph metrics mapped primarily onto the ventral attention network (65), an aggregate of the salience network (75) and the site of the strongest effects of oxytocin on timeseries connectivity in a previous report (46). Considering that our results were derived after collapsing across healthy controls and CHR-P individuals, effects of oxytocin within the ventral attention network, brainstem and other regions found here could be said to reflect common effects that operate irrespective of clinical status.

**Group x Treatment Interaction Effects**

Our major—and to our knowledge, novel—finding was the presence of widespread interaction effects across all local graph metrics and across a multitude of brain regions, suggesting that oxytocin modulates network properties in a clinical status-specific manner. This is consistent with the differential effects of oxytocin on timeseries correlational connectivity reported in a variety of clinical populations vs healthy controls, including patients with social anxiety (47,76), post-traumatic stress disorder (48), and autism (49). Here we demonstrate, for the first time,

that this is also the case in terms of effects on functional brain network topology in people at CHR-P.

Strikingly, oxytocin was found to have divergent effects on local topology in core regions implicated in the pathophysiology of psychosis, including betweenness-centrality of the thalamus and striatum (pallidum, nucleus accumbens [NAcc]), and local efficiency of the entorhinal cortex. In all of these regions except the NAcc, graph metrics were relatively lower in CHR-P individuals under placebo and were increased by oxytocin, with the reverse relationship seen in controls. The thalamus, hippocampus and striatum (including pallidum and NAcc) represent key components of the most influential circuit models of psychosis, which propose that hippocampal hyperactivation drives downstream striatal hyperdopaminergia via increased excitation of the NAcc, increased inhibition of ventral pallidum and thus reduced inhibition of midbrain/VTA dopamine neurons projecting to the NAcc and associative striatum (16–18,77). Given the well-established dysfunction within these regions in psychosis, one possibility is that oxytocin's effects differ as a function of baseline network (dis)organisation. Nonpsychotic first-degree relatives have abnormal anatomic centrality in many of the regions reported here, including the pallidum, thalamus and hippocampus (78). Although we did not find significant effects in the hippocampus directly, the entorhinal cortex is part of the hippocampal formation and acts as a multilevel buffer, bi-directionally gating information flow between neocortex and hippocampus (79). Reduced nodal clustering has been observed in the hippocampus, thalamus and amygdala in CHR-P transitions vs non-transitions and controls (6), and adolescent-onset schizophrenia patients show decreased nodal efficiency and strength within highly integrative network hubs, most consistently in the hippocampal formation (2). Transition to psychosis is also associated with reduced thalamic efficiency (6) and thalamocortical dysconnectivity more broadly (21). If, as this evidence suggests, network topology is altered in CHR-P individuals, it is conceivable that the net effects of exogenously administered oxytocin on network organisation may well differ, even if its cognitive-behavioural effects are still geared towards optimised tuning of social salience/attentional orientation (80). Such interaction effects would echo those seen among the wider connectivity literature (81,82) where the greatest magnitude of the connectomic, cognitive and/or behavioural effects of oxytocin are often reported in those subjects with the greatest divergence (compared to controls) at baseline/under placebo (47,82).

Albeit in the context of interactions, in contrast to the other subcortical interaction effects we found relatively *greater* centrality of the NAcc in the CHR-P group under placebo, a region previously identified as a locus of CHR-associated structural rich-club dysfunction (83). The NAcc is also the terminus for dopamine neurons projecting from the midbrain/VTA (84) in the

above-mentioned psychosis-linked circuit. Although speculative, our finding that in CHR-P patients, oxytocin decreased the centrality of the NAcc but increased centrality of the pallidum (which provides inhibition of the VTA) may suggest that oxytocin affects network properties—in mesolimbic dopamine pathway regions—in a psychosis risk-selective manner, and in a direction that ameliorates baseline dysfunction. Indeed, engagement of dopaminergic circuits seems to be a key locus for some of the effects of oxytocin (85) (for a review see (86)) and a wealth of evidence demonstrates interplay of the dopamine and oxytocin systems (87–92).

A further potential contributor to the differential effects of oxytocin is perturbations in the endogenous oxytocin system itself. Although direct and robust evidence for altered receptor number/distribution (and central/peripheral levels of oxytocin) is lacking, various stands of indirect evidence suggest that the oxytocin system is dysfunctional in psychosis (93) and is associated with symptom profiles (92), amygdala activation (94), susceptibility to psychosis, anhedonia-asociality and striatal-amygdala network connectivity (95). Overall, psychosis risk-related differences in network topology, dopamine function, the oxytocin system, as well as alterations in the set-points of other circuits are not mutually exclusive and may each contribute to the differential net effects of oxytocin on graph properties observed here.

**Limitations**

A number of limitations warrant consideration. First, data from CHR-P and healthy control groups were from different studies that had slightly different experimental designs, with the controls participating in a triple-dummy study (using multiple administration methods on all occasions) and CHR-P subjects participating in a simple oxytocin vs placebo nasal spray challenge. While the two studies were conceived together specifically to ensure that their data could be combined for the present analyses, it is possible that residual effects from differing designs could underlie some of the group differences we observed. Second, a number of the clinical and demographic variables collected in the CHR-P group were not collected in controls. As such, we did not control for these potential confounders within the analyses. While there were no significant between-group differences for most key demographic factors, there were more smokers in the CHR-P relative to the control group. The within-subject element helped to mitigate the potential impact of this but we cannot rule out an effect on our between-group results. Our sample size was relatively large for pharmaco-MRI study including a CHR-P sample, but a recent paper on the reliability of graph analytic results suggested that sample sizes of more than 80 are needed (96). However, as well as collecting multi-echo data we used a rigorous denoising protocol with enhanced quality control procedures, a combination that has been shown to perform favourably in terms of signal-to-noise ratio compared to other denoising pipelines (57). We further sought to maximise reliability of our findings by using

weighted graphs and metrics summarised (using AUC) across multiple cost functions. Finally, we excluded female subjects due to sexual dimorphism in oxytocinergic function (97,98) and studied only one (mid-to-high range) dose of oxytocin. In light of the now well-known dose-dependent neurophysiological properties of oxytocin (99), differential connectomic effects by dose and gender should be explored in future studies.

**Conclusions**

Collectively, our findings provide new insights on aberrant functional brain network organisation associated with psychosis risk and demonstrate, for the first time, that oxytocin modulates network topology in brain regions implicated in the pathophysiology of psychosis in a clinical status-specific manner. Given the current lack of effective treatments for people at CHR-P, a deeper understanding of how functional connectomic alterations contribute to psychosis risk and onset, and the potential ameliorative effects of experimental therapeutics such as oxytocin, remain important avenues for future research.

## Disclosures

*Funding:* This work was supported by the National Institute for Health Research (NIHR) Biomedical Research Centre (BRC) at South London and Maudsley NHS Foundation Trust and King's College London (PFP, PMc, YP, DM); by a Brain & Behaviour Research Foundation NARSAD Award (grant number 22593 to PFP); an Economic and Social Research Council Grant (ES/K009400/1 to YP); by an unrestricted research grant by PARI GmbH to YP; and by the Department of Psychosis Studies, Institute of Psychiatry, Psychology & Neuroscience, King's College London. RAM's work was supported by a NIHR Clinical Lectureship and a Wellcome Trust Clinical Research Career Development Fellowship. The views expressed are those of the authors and not necessarily those of the NHS, the NIHR or the Department of Health and Social Care. The funders had no influence on the design, collection, analysis and interpretation of the data, writing of the report and decision to submit this article for publication.

*Conflict of Interest:* PFP has received research funds or personal fees from Lundbeck, Angelini, Menarini, Sunovion, Boehringer Ingelheim and Proxymm Science outside of the current study. RAM has received honoraria for educational talks sponsored by Otsuka and Janssen. The authors have declared that there are no conflicts of interest in relation to the subject of this study.

## Acknowledgements

The authors wish to thank the study volunteers for their participation, members of the OASIS and THEDS clinical teams, and the radiographers at the Centre for Neuroimaging Sciences, King's College London, who carried out the MRI scans.

## Author Contributions

Substantial contributions to conception and design (PFP, YP, PMc, SW, FZ, PA, SS), acquisition of data (CD, DM, AdM, VRC, UP, GR, MC, DO), analysis (CD, DM, OD) and interpretation of data (CD, DM, RAM), drafting of the article (CD, DM) or revising it critically for important intellectual content (all authors), study supervision (PFP, YP, PMc), acquisition of funding (PFP, YP, PMc, PMo, SS, DT, PA, FZ, SW), final approval of the version to be published (all authors).

## Supplementary Information

Supplementary Material is attached.

## REFERENCES

1. Collin G, Keshavan MS. Connectome development and a novel extension to the neurodevelopmental model of schizophrenia. Dialogues in Clinical Neuroscience. 2018;20(2):101–11.

2. Li M, Becker B, Zheng J, Zhang Y, Chen H, Liao W, et al. Dysregulated maturation of the functional connectome in antipsychotic-naïve, first-episode patients with adolescent-onset schizophrenia. Schizophrenia Bulletin. 2019;45(3):689–97.

3. Morgan SE, Young J, Patel AX, Whitaker KJ, Scarpazza C, van Amelsvoort T, et al. Functional Magnetic Resonance Imaging Connectivity Accurately Distinguishes Cases With Psychotic Disorders From Healthy Controls, Based on Cortical Features Associated With Brain Network Development. Biological Psychiatry: Cognitive Neuroscience and Neuroimaging. 2021;6(12):1125–34.

4. Collin G, Seidman LJ, Keshavan MS, Stone WS, Qi Z, Zhang T, et al. Functional connectome organization predicts conversion to psychosis in clinical high-risk youth from the SHARP program. Molecular Psychiatry. 2020;25(10):2431–40.

5. Lord LD, Allen P, Expert P, Howes O, Broome M, Lambiotte R, et al. Functional brain networks before the onset of psychosis: A prospective fMRI study with graph theoretical analysis. NeuroImage: Clinical. 2012;1(1):91–8.

6. Wang C, Lee J, Ho NF, Lim JKW, Poh JS, Rekhi G, et al. Large-scale network topology reveals heterogeneity in individuals with at risk mental state for psychosis: Findings from the longitudinal youth-at-risk study. Cerebral Cortex. 2018;28(12):4234–43.

7. Fusar-Poli P, Salazar De Pablo G, Correll CU, Meyer-Lindenberg A, Millan MJ, Borgwardt S, et al. Prevention of Psychosis: Advances in Detection, Prognosis, and Intervention. JAMA Psychiatry. 2020;77(7):755–65.

8. Salazar De Pablo G, Radua J, Pereira J, Bonoldi I, Arienti V, Besana F, et al. Probability of Transition to Psychosis in Individuals at Clinical High Risk: An Updated Meta-analysis. JAMA Psychiatry. 2021;78(9):970–8.

9. Davies C, Cipriani A, Ioannidis JPA, Radua J, Stahl D, Provenzani U, et al. Lack of evidence to favor specific preventive interventions in psychosis: a network meta-analysis. World Psychiatry. 2018 Jun;17(2):196–209.

10. Davies C, Radua J, Cipriani A, Stahl D, Provenzani U, McGuire P, et al. Efficacy and Acceptability of Interventions for Attenuated Positive Psychotic Symptoms in Individuals at Clinical High Risk of Psychosis: A Network Meta-Analysis. Frontiers in Psychiatry. 2018 Jun 12;9(JUN):1–17.

11. Allen P, Chaddock CA, Egerton A, Howes OD, Bonoldi I, Zelaya F, et al. Resting hyperperfusion of the hippocampus, midbrain, and basal ganglia in people at high risk for psychosis. American Journal of Psychiatry. 2016;173(4):392–9.

12. Allen P, Luigjes J, Howes OD, Egerton A, Hirao K, Valli I, et al. Transition to psychosis associated with prefrontal and subcortical dysfunction in ultra high-risk individuals. Schizophrenia Bulletin. 2012;38(6):1268–76.

13. Jalbrzikowski M, Hayes RA, Wood SJ, Nordholm D, Zhou JH, Fusar-Poli P, et al. Association of Structural Magnetic Resonance Imaging Measures with Psychosis

Onset in Individuals at Clinical High Risk for Developing Psychosis: An ENIGMA Working Group Mega-analysis. JAMA Psychiatry. 2021;78(7):753–66.

14. Lieberman JA, Small SA, Girgis RR. Early detection and preventive intervention in schizophrenia: From fantasy to reality. American Journal of Psychiatry. 2019;176(10):794–810.

15. Andreou C, Borgwardt S. Structural and functional imaging markers for susceptibility to psychosis. Molecular Psychiatry. 2020;25(11):2773–85.

16. Lisman JE, Coyle JT, Green RW, Javitt DC, Benes FM, Heckers S, et al. Circuit-based framework for understanding neurotransmitter and risk gene interactions in schizophrenia. Trends in Neurosciences. 2008;31(5):234–42.

17. Grace AA, Gomes F V. The Circuitry of Dopamine System Regulation and its Disruption in Schizophrenia: Insights Into Treatment and Prevention. Schizophrenia Bulletin. 2019 Jan 1;45(1):148–57.

18. Dandash O, Pantelis C, Fornito A. Dopamine, fronto-striato-thalamic circuits and risk for psychosis. Schizophrenia Research. 2017;180:48–57.

19. Fornito A, Harrison BJ, Goodby E, Dean A, Ooi C, Nathan PJ, et al. Functional dysconnectivity of corticostriatal circuitry as a risk phenotype for psychosis. JAMA Psychiatry. 2013;70(11):1143–51.

20. Colibazzi T, Yang Z, Horga G, Yan CG, Corcoran CM, Klahr K, et al. Aberrant Temporal Connectivity in Persons at Clinical High Risk for Psychosis. Biological Psychiatry: Cognitive Neuroscience and Neuroimaging. 2017;2(8):696–705.

21. Anticevic A, Haut K, Murray JD, Repovs G, Yang GJ, Diehl C, et al. Association of Thalamic Dysconnectivity and Conversion to Psychosis in Youth and Young Adults at Elevated Clinical Risk. JAMA Psychiatry. 2015;72(9):882–91.

22. O'Neill A, Mechelli A, Bhattacharyya S. Dysconnectivity of Large-Scale Functional Networks in Early Psychosis: A Meta-analysis. Schizophrenia Bulletin. 2018;(July):1–12.

23. Wotruba D, Michels L, Buechler R, Metzler S, Theodoridou a, Gerstenberg M, et al. Aberrant Coupling Within and Across the Default Mode, Task-Positive, and Salience Network in Subjects at Risk for Psychosis. Schizophrenia Bulletin. 2013;1–10.

24. Del Fabro L, Schmidt A, Fortea L, Delvecchio G, D'Agostino A, Radua J, et al. Functional brain network dysfunctions in subjects at high-risk for psychosis: A meta-analysis of resting-state functional connectivity. Neuroscience and Biobehavioral Reviews. 2021;128(June):90–101.

25. Watts DJ, Strogatz SH. Collective dynamics of 'small-world' networks. Nature. 1998 Jun;393(6684):440–2.

26. Bullmore ET, Bassett DS. Brain graphs: Graphical models of the human brain connectome. Annual Review of Clinical Psychology. 2011;7:113–40.

27. Fornito A, Zalesky A, Pantelis C, Bullmore ET. Schizophrenia, neuroimaging and connectomics. NeuroImage. 2012;62(4):2296–314.

28. Rubinov M, Sporns O. Complex network measures of brain connectivity: Uses and interpretations. NeuroImage. 2010;52(3):1059–69.

29. Collin G, Scholtens LH, Kahn RS, Hillegers MHJ, van den Heuvel MP. Affected Anatomical Rich Club and Structural–Functional Coupling in Young Offspring of Schizophrenia and Bipolar Disorder Patients. Biological Psychiatry. 2017;82(10):746–55.

30. Friston K, Brown HR, Siemerkus J, Stephan KE. The dysconnection hypothesis (2016). Schizophrenia Research. 2016;176(2–3):83–94.

31. Kambeitz J, Kambeitz-Ilankovic L, Cabral C, Dwyer DB, Calhoun VD, Van Den Heuvel MP, et al. Aberrant Functional Whole-Brain Network Architecture in Patients with Schizophrenia: A Meta-analysis. Schizophrenia Bulletin. 2016;42(1):S13–21.

32. Liu Y, Liang M, Zhou Y, He Y, Hao Y, Song M, et al. Disrupted small-world networks in schizophrenia. Brain. 2008;131(4):945–61.

33. Lynall ME, Bassett DS, Kerwin R, McKenna PJ, Kitzbichler M, Muller U, et al. Functional connectivity and brain networks in schizophrenia. Journal of Neuroscience. 2010;30(28):9477–87.

34. Alexander-Bloch AF, Gogtay N, Meunier D, Birn R, Clasen L, Lalonde F, et al. Disrupted modularity and local connectivity of brain functional networks in childhood-onset schizophrenia. Frontiers in Systems Neuroscience. 2010;4(October):1–16.

35. Jalbrzikowski M, Liu F, Foran W, Roeder K, Devlin B, Luna B. Resting-State Functional Network Organization Is Stable across Adolescent Development for Typical and Psychosis Spectrum Youth. Schizophrenia Bulletin. 2020;46(2):395–407.

36. Smith AS, Tabbaa M, Lei K, Eastham P, Butler MJ, Linton L, et al. Local oxytocin tempers anxiety by activating GABAA receptors in the hypothalamic paraventricular nucleus. Psychoneuroendocrinology. 2016;63:50–8.

37. Meyer-Lindenberg A, Domes G, Kirsch P, Heinrichs M. Oxytocin and vasopressin in the human brain: social neuropeptides for translational medicine. Nature reviews Neuroscience. 2011;12(9):524–38.

38. Yao S, Becker B, Zhao W, Zhao Z, Kou J, Ma X, et al. Oxytocin modulates attention switching between interoceptive signals and external social cues. Neuropsychopharmacology. 2018;43(2):294–301.

39. Guastella AJ, Mitchell PB, Mathews F. Oxytocin Enhances the Encoding of Positive Social Memories in Humans. Biological Psychiatry. 2008;64(3):256–8.

40. Domes G, Heinrichs M, Michel A, Berger C, Herpertz SC. Oxytocin Improves ‘Mind-Reading’ in Humans. Biological Psychiatry. 2007;61(6):731–3.

41. Martins D, Davies C, Micheli A De, Oliver D, Fusar-poli P, Paloyelis Y. Intranasal oxytocin increases heart-rate variability in men at clinical high risk for psychosis : a proof-of-concept study. Translational Psychiatry. 2020;

42. Schmidt A, Davies C, Paloyelis Y, Meyer N, De Micheli A, Ramella-Cravaro V, et al. Acute oxytocin effects in inferring others’ beliefs and social emotions in people at clinical high risk for psychosis. Translational Psychiatry. 2020 Dec 22;10(1):203.

43. Davies C, Rutigliano G, De Micheli A, Stone JM, Ramella-Cravaro V, Provenzani U, et al. Neurochemical effects of oxytocin in people at clinical high risk for psychosis. European Neuropsychopharmacology. 2019 May;29(5):601–15.

44. Davies C, Paloyelis Y, Rutigliano G, Cappucciati M, De Micheli A, Ramella-Cravaro V, et al. Oxytocin modulates hippocampal perfusion in people at clinical high risk for psychosis. Neuropsychopharmacology. 2019 Jun 9;44(7):1300–9.

45. Xin F, Zhou F, Zhou X, Ma X, Geng Y, Zhao W, et al. Oxytocin Modulates the Intrinsic Dynamics Between Attention-Related Large-Scale Networks. Cerebral Cortex. 2018;1–13.

46. Brodmann K, Gruber O, Goya-Maldonado R. Intranasal Oxytocin Selectively Modulates Large-Scale Brain Networks in Humans. Brain Connectivity. 2017;7(7):brain.2017.0528.

47. Dodhia S, Hosanagar A, Fitzgerald D a, Labuschagne I, Wood AG, Nathan PJ, et al. Modulation of Resting-State Amygdala-Frontal Functional Connectivity by Oxytocin in Generalized Social Anxiety Disorder. Neuropsychopharmacology. 2014 Aug 5;39(9):2061–9.

48. Koch SB, van Zuiden M, Nawijn L, Frijling JL, Veltman DJ, Olff M. Intranasal Oxytocin Normalizes Amygdala Functional Connectivity in Post-Traumatic Stress Disorder. Neuropsychopharmacology. 2016;41(January):1–34.

49. Procyshyn TL, Lombardo M V, Lai MC, Jassim N, Auyeung B, Crockford SK, et al. Oxytocin Enhances Basolateral Amygdala Activation and Functional Connectivity While Processing Emotional Faces: Preliminary Findings in Autistic Versus Non-Autistic Women. Social Cognitive and Affective Neuroscience. 2022 Mar 7;1–33.

50. Martins D, Dipasquale O, Paloyelis Y. Oxytocin modulates local topography of human functional connectome in healthy men at rest. Communications Biology. 2021 Dec 15;4(1):68.

51. Fusar-Poli P, Spencer T, De Micheli A, Curzi V, Nandha S, McGuire P. Outreach and support in South-London (OASIS) 2001—2020: Twenty years of early detection, prognosis and preventive care for young people at risk of psychosis. European Neuropsychopharmacology. 2020;39:111–22.

52. Yung AR, Pan Yuen H, McGorry PD, Phillips LJ, Kelly D, Dell'olio M, et al. Mapping the Onset of Psychosis: The Comprehensive Assessment of At-Risk Mental States. Australian & New Zealand Journal of Psychiatry. 2005 Nov 17;39(11–12):964–71.

53. Guastella AJ, Hickie IB, McGuinness MM, Otis M, Woods EA, Disinger HM, et al. Recommendations for the standardisation of oxytocin nasal administration and guidelines for its reporting in human research. Psychoneuroendocrinology. 2013;38(5):612–25.

54. Paloyelis Y, Doyle OM, Zelaya FO, Maltezos S, Williams SC, Fotopoulou A, et al. A Spatiotemporal Profile of In Vivo Cerebral Blood Flow Changes Following Intranasal Oxytocin in Humans. Biological Psychiatry. 2016;79(8):693–705.

55. Cox RW. AFNI: Software for Analysis and Visualization of Functional Magnetic Resonance Neuroimages. Computers and Biomedical Research. 1996 Jun;29(3):162–73.

56. Kundu P, Brenowitz ND, Voon V, Worbe Y, Vértes PE, Inati SJ, et al. Integrated strategy for improving functional connectivity mapping using multiecho fMRI. Proceedings of the National Academy of Sciences of the United States of America. 2013;110(40):16187–92.

57. Dipasquale O, Sethi A, Lagan MM, Baglio F, Baselli G, Kundu P, et al. Comparing resting state fMRI de-noising approaches using multi-and single-echo acquisitions. PLoS ONE. 2017;12(3):1–25.

58. Desikan RS, Ségonne F, Fischl B, Quinn BT, Dickerson BC, Blacker D, et al. An automated labeling system for subdividing the human cerebral cortex on MRI scans into gyral based regions of interest. NeuroImage. 2006;31(3):968–80.

59. van den Heuvel MP, de Lange SC, Zalesky A, Seguin C, Yeo BTT, Schmidt R. Proportional thresholding in resting-state fMRI functional connectivity networks and consequences for patient-control connectome studies: Issues and recommendations. NeuroImage. 2017;152(February):437–49.

60. Achard S, Bullmore E. Efficiency and cost of economical brain functional networks. PLoS Computational Biology. 2007;3(2):0174–83.

61. Zhang J, Wang J, Wu Q, Kuang W, Huang X, He Y, et al. Disrupted brain connectivity networks in drug-naive, first-episode major depressive disorder. Biological Psychiatry. 2011;70(4):334–42.

62. Xu T, Cullen KR, Mueller B, Schreiner MW, Lim KO, Schulz SC, et al. Network analysis of functional brain connectivity in borderline personality disorder using resting-state fMRI. NeuroImage: Clinical. 2016;11:302–15.

63. Zalesky A, Fornito A, Bullmore ET. Network-based statistic: Identifying differences in brain networks. NeuroImage. 2010;53(4):1197–207.

64. Larivière S, Paquola C, Park B yong, Royer J, Wang Y, Benkarim O, et al. The ENIGMA Toolbox: multiscale neural contextualization of multisite neuroimaging datasets. Nature Methods. 2021;18(7):698–700.

65. Yeo BTT, Krienen FM, Sepulcre J, Sabuncu MR, Lashkari D, Hollinshead M, et al. The organization of the human cerebral cortex estimated by intrinsic functional connectivity. Journal of Neurophysiology. 2011;106(3):1125–65.

66. Satterthwaite TD, Baker JT. How can studies of resting-state functional connectivity help us understand psychosis as a disorder of brain development? Current Opinion in Neurobiology. 2015;30(October 2014):85–91.

67. Schmidt A, Diwadkar VA, Smieskova R, Harrisberger F, Lang UE, McGuire P, et al. Approaching a network connectivity-driven classification of the psychosis continuum: A selective review and suggestions for future research. Frontiers in Human Neuroscience. 2015;8(JAN):1–16.

68. Baker JT, Dillon DG, Patrick LM, Roffman JL, Brady RO, Pizzagalli DA, et al. Functional connectomics of affective and psychotic pathology. Proceedings of the National Academy of Sciences of the United States of America. 2019;116(18):9050–9.

69. Marek S, Dosenbach NUF. The frontoparietal network: function, electrophysiology, and importance of individual precision mapping. Dialogues in Clinical Neuroscience. 2018 Jun 30;20(2):133–40.

70. Sha Z, Wager TD, Mechelli A, He Y. Common Dysfunction of Large-Scale Neurocognitive Networks Across Psychiatric Disorders. Biological Psychiatry. 2019;85(5):379–88.

71. Freeman LC. Centrality in social networks. Social Networks. 1979;1(3):215–39.

72. Rosenfeld AJ, Lieberman JA, Jarskog LF. Oxytocin, dopamine, and the amygdala: A neurofunctional model of social cognitive deficits in schizophrenia. Schizophrenia Bulletin. 2011;37(5):1077–87.

73. Shamay-Tsoory SG, Abu-Akel A. The Social Salience Hypothesis of Oxytocin. Biological Psychiatry. 2015;79(26):1–9.

74. Redgrave P, Gurney K. The short-latency dopamine signal: A role in discovering novel actions? Nature Reviews Neuroscience. 2006;7(12):967–75.

75. Uddin LQ, Yeo BTT, Spreng RN. Towards a Universal Taxonomy of Macro-scale Functional Human Brain Networks. Brain Topography. 2019;32(6):926–42.

76. Gorka SM, Fitzgerald D a, Labuschagne I, Hosanagar A, Wood AG, Nathan PJ, et al. Oxytocin Modulation of Amygdala Functional Connectivity to Fearful Faces in Generalized Social Anxiety Disorder. Neuropsychopharmacology. 2014;40(April):1–31.

77. Modinos G, Allen P, Grace AA, McGuire P. Translating the MAM model of psychosis to humans. Trends in Neurosciences. 2015;38(3):129–38.

78. Zhang W, Lei D, Keedy SK, Ivleva EI, Eum S, Yao L, et al. Brain gray matter network organization in psychotic disorders. Neuropsychopharmacology. 2020;45(4):666–74.

79. Small SA, Schobel SA, Buxton RB, Witter MP, Barnes CA. A pathophysiological framework of hippocampal dysfunction in ageing and disease. Nature Reviews Neuroscience. 2011;12(10):585–601.

80. Ma Y, Shamay-Tsoory S, Han S, Zink CF. Oxytocin and Social Adaptation: Insights from Neuroimaging Studies of Healthy and Clinical Populations. Trends in Cognitive Sciences. 2016;20(2):133–45.

81. Choe KY, Bethlehem RAI, Safrin M, Dong H, Salman E, Li Y, et al. Oxytocin normalizes altered circuit connectivity for social rescue of the Cntnap2 knockout mouse. Neuron. 2021;1–14.

82. Abram S V, De Coster L, Roach BJ, Mueller BA, van Erp TGM, Calhoun VD, et al. Oxytocin Enhances an Amygdala Circuit Associated With Negative Symptoms in Schizophrenia: A Single-Dose, Placebo-Controlled, Crossover, Randomized Control Trial. Schizophrenia Bulletin. 2019;

83. Schmidt A, Crossley NA, Harrisberger F, Smieskova R, Lenz C, Riecher-Rössler A, et al. Structural network disorganization in subjects at clinical high risk for psychosis. Schizophrenia Bulletin. 2017;43(3):583–91.

84. McCutcheon RA, Abi-dargham A, Howes OD. Schizophrenia, Dopamine and the Striatum: From Biology to Symptoms. Trends in Neurosciences. 2019;xx:(1-12).

85. Hung LW, Neuner S, Polepalli JS, Beier KT, Wright M, Walsh JJ, et al. Gating of social reward by oxytocin in the ventral tegmental area. Science. 2017;357(6358):1406–11.

86. Love TM. Oxytocin, motivation and the role of dopamine. Pharmacology Biochemistry and Behavior. 2014;119:49–60.

87. Rokicki J, Kaufmann T, de Lange AMG, van der Meer D, Bahrami S, Sartorius AM, et al. Oxytocin receptor expression patterns in the human brain across development. Neuropsychopharmacology. 2022 Jul 28;47(8):1550–60.

88. Quintana DS, Rokicki J, van der Meer D, Alnæs D, Kaufmann T, Córdova-Palomera A, et al. Oxytocin pathway gene networks in the human brain. Nature Communications. 2019 Dec 8;10(1):668.

89. Romero-Fernandez W, Borroto-Escuela DO, Agnati LF, Fuxe K. Evidence for the existence of dopamine d2-oxytocin receptor heteromers in the ventral and dorsal striatum with facilitatory receptor–receptor interactions. Molecular Psychiatry. 2012;18(8):849–50.

90. Love TM, Enoch MA, Hodgkinson CA, Peciña M, Mickey B, Koeppe RA, et al. Oxytocin gene polymorphisms influence human dopaminergic function in a sex-dependent manner. Biological Psychiatry. 2012;72(3):198–206.

91. Chang WH, Lee IH, Chen KC, Chi MH, Chiu NT, Yao WJ, et al. Oxytocin receptor gene rs53576 polymorphism modulates oxytocin-dopamine interaction and neuroticism traits-A SPECT study. Psychoneuroendocrinology. 2014;47:212–20.

92. Montag C, Brockmann EM, Bayerl M, Rujescu D, Müller DJ, Gallinat J. Oxytocin and oxytocin receptor gene polymorphisms and risk for schizophrenia: A case-control study. The world journal of biological psychiatry : the official journal of the World Federation of Societies of Biological Psychiatry. 2012;2975(July 2011):1–9.

93. Shilling PD, Feifel D. Potential of Oxytocin in the Treatment of Schizophrenia. CNS Drugs. 2016;30(3):193–208.

94. Haram M, Bettella F, Brandt CL, Quintana DS, Nerhus M, Bjella T, et al. Contribution of oxytocin receptor polymorphisms to amygdala activation in schizophrenia spectrum disorders. BJPsych Open. 2016 Nov 2;2(6):353–8.

95. Bang M, Kang JI, Kim SJ, Park JY, Kim KR, Lee SY, et al. Reduced DNA Methylation of the Oxytocin Receptor Gene Is Associated with Anhedonia-Asociality in Women with Recent-Onset Schizophrenia and Ultra-high Risk for Psychosis. Schizophrenia Bulletin. 2019;45(6):1279–90.

96. Termenon M, Jaillard A, Delon-Martin C, Achard S. Reliability of graph analysis of resting state fMRI using test-retest dataset from the Human Connectome Project. NeuroImage. 2016;142:172–87.

97. Rilling JK, DeMarco AC, Hackett PD, Chen X, Gautam P, Stair S, et al. Sex differences in the neural and behavioral response to intranasal oxytocin and vasopressin during human social interaction. Psychoneuroendocrinology. 2014;39(1):237–48.

98. Wigton R, Radua J, Allen P, Averbeck B, Meyer-Lindenberg A, McGuire P, et al. Neurophysiological effects of acute oxytocin administration: systematic review and meta-analysis of placebo-controlled imaging studies. Journal of Psychiatry & Neuroscience. 2015 Jan 1;40(1):E1–22.

99. Martins D, Brodmann K, Veronese M, Dipasquale O, Mazibuko N, Schuschnig U, et al. “Less is more”: A dose-response account of intranasal oxytocin pharmacodynamics in the human brain. Progress in Neurobiology. 2022;211(January):102239.

100. Alexander-Bloch AF, Shou H, Liu S, Satterthwaite TD, Glahn DC, Shinohara RT, et al. On testing for spatial correspondence between maps of human brain structure and function. NeuroImage. 2018;178(February):540–51.

# TABLES

## TABLE 1. Participant Demographic and Clinical Characteristics

| Variable | CHR-P (N=30) | Controls (N=17) | Statistics |
|---|---|---|---|
| Age, years; mean (SD) | 23.2 (4.7) | 24.2 (5.3) | p = .51 [c] |
| Sex, N (%) male | 30 (100) | 17 (100) | N/A [d] |
| Ethnicity, N White/Black/Asian/Mixed | 16/6/4/4 | – | – |
| Handedness, N (%) right | 26 (87) | 17 (100) | p = .15 [e] |
| Education, years; mean (SD) | 13.2 (1.9) [g] | – [g] | – |
| CHR-P Subtype[a], N BLIPS/APS/GRD | 6/23/1 | N/A | N/A |
| CAARMS positive symptoms[b]; mean (SD) | 11.7 (3.3) | N/A | N/A |
| GF social score; mean (SD) | 6.8 (1.5) | N/A | N/A |
| GF role score; mean (SD) | 7.0 (1.7) | N/A | N/A |
| Current smoker, N (%) yes | 17 (57) | 4 (24) | **p = .028** [f] |
| Cigarettes/day; mean (SD) | 9.8 (6.0) | 4.5 (4.0) | p = .12 [c] |
| Cannabis ever used, N (%) yes | 24 (80) | 10 (59) | p = .18 [e] |
| Current alcohol use, N (%) yes | 26 (87) | 16 (94) | p = .64 [e] |

[a] Comprehensive Assessment of At-Risk Mental States (CAARMS) subgroup, BLIPS Brief Limited Intermittent Psychotic Symptoms; APS Attenuated Psychotic Symptoms; GRD Genetic Risk and Deterioration. [b] Sum of the global (severity) ratings for positive subscale items (P1-P4) of the CAARMS. GF - Global Functioning (Role and Social) Scale. [c] independent t-test, [d] no statistical test necessary, [e] Fisher's Exact test, [f] chi-square test, [g] the majority of controls were university students (approximately between 13-16 years of education), whereas 43% of CHR-P were university students or had completed a degree - of the remaining CHR-P subjects, 27% were currently undertaking A-Levels/BTEC (11-13 years of education), 20% were in full-time or part-time work, and 10% were unemployed.

## TABLE 2. Effects of group, treatment and interaction effects on nodal betweenness-centrality, degree and local efficiency

| GROUP EFFECTS | | | |
|---|---|---|---|
| **Node** | **Direction** | **T statistic** | **P (FDR-corr)** |
| **Betweenness-Centrality** | | | |
| Caudal middle frontal gyrus, left | HC > CHR | -2.165 | 0.036 |
| Insula, left | HC > CHR | -2.236 | 0.031 |
| Inferior temporal gyrus, right | CHR > HC | 2.150 | 0.037 |
| Superior temporal gyrus, right | CHR > HC | 2.092 | 0.042 |
| **Node degree** | | | |
| Lingual gyrus, left | HC > CHR | -2.217 | 0.032 |
| Lateral orbital frontal cortex, right | CHR > HC | 2.757 | 0.009 |
| Pars triangularis, right | CHR > HC | 2.353 | 0.023 |
| **Local Efficiency** | | | |
| Pericalcarine cortex, left | CHR > HC | 2.451 | 0.018 |
| Rostral middle frontal gyrus, left | CHR > HC | 3.896 | <0.001 |
| Pars orbitalis, right | CHR > HC | 2.698 | 0.010 |
| Pericalcarine cortex, right | CHR > HC | 2.125 | 0.039 |
| Rostral middle frontal gyrus, right | CHR > HC | 2.142 | 0.038 |
| **TREATMENT EFFECTS** | | | |
| **Node** | **Direction** | **T statistic** | **P (FDR-corr)** |
| **Betweenness-Centrality** | | | |
| Brainstem | OT > PL | 2.337 | 0.024 |
| Supramarginal gyrus, left | PL > OT | -2.249 | 0.030 |
| Insula, right | PL > OT | -3.286 | 0.002 |
| **Node degree** | | | |
| Precentral gyrus, left | OT > PL | 2.885 | 0.006 |
| **Local Efficiency** | | | |
| Paracentral lobule, left | OT > PL | 2.699 | 0.010 |
| Paracentral lobule, right | OT > PL | 2.652 | 0.011 |
| Pars opercularis, right | OT > PL | 2.600 | 0.013 |
| **INTERACTION EFFECTS** | | | |
| **Node** | **Direction** | **T statistic*** | **P (FDR-corr)** |
| **Betweenness-Centrality** | | | |
| Precentral gyrus, right | OT > PL in CHR; OT < PL in HC | 2.062 | 0.045 |
| Thalamus, left | OT > PL in CHR; OT < PL in HC | 2.059 | 0.046 |
| Pallidum, right | OT > PL in CHR; OT < PL in HC | 2.785 | 0.008 |
| Precuneus cortex, left | OT < PL in CHR; OT > PL in HC | -3.387 | 0.002 |
| Superior frontal gyrus, left | OT < PL in CHR; OT > PL in HC | -2.561 | 0.014 |
| Accumbens, left | OT < PL in CHR; OT > PL in HC | -2.490 | 0.017 |
| **Node degree** | | | |
| Precuneus cortex, left | OT < PL in CHR; OT > PL in HC | -2.437 | 0.019 |
| Superior frontal gyrus, left | OT < PL in CHR; OT > PL in HC | -2.139 | 0.038 |
| **Local Efficiency** | | | |
| Entorhinal cortex, left | OT > PL in CHR; OT < PL in HC | 2.247 | 0.030 |
| Entorhinal cortex, right | OT > PL in CHR; OT < PL in HC | 2.633 | 0.012 |
| Temporal pole, right | OT > PL in CHR; OT < PL in HC | 2.102 | 0.041 |
| Pericalcarine cortex, left | OT < PL in CHR; OT > PL in HC | -2.061 | 0.045 |

***Footnotes***: FDR-corr indicates FDR-corrected P-values. *Interaction t-test compared difference values (oxytocin minus placebo) between groups. OT, oxytocin; PL, placebo; CHR, Clinical High Risk for Psychosis; HC, healthy control.

# FIGURES

**FIGURE 1.** Overview of the network analysis steps.

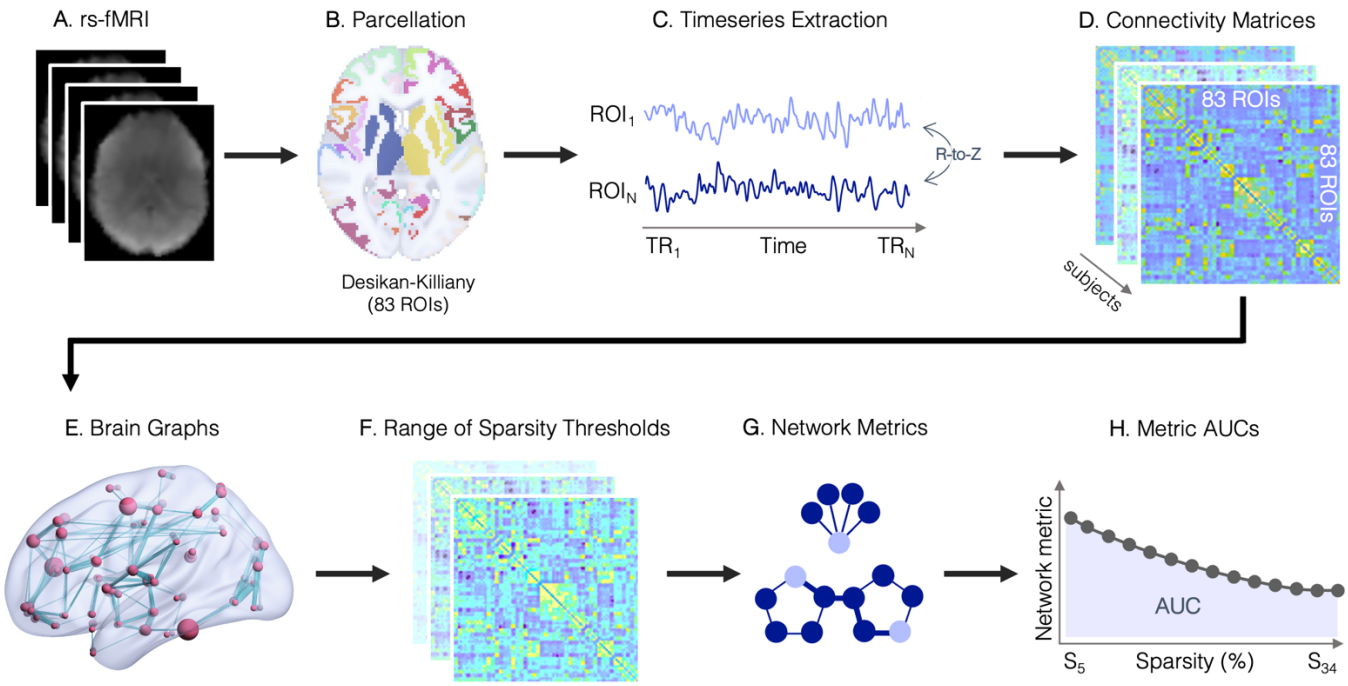

**FIGURE 2.** Overview of group, treatment and interaction effects across all nodal metrics (betweenness-centrality, node degree and local efficiency).

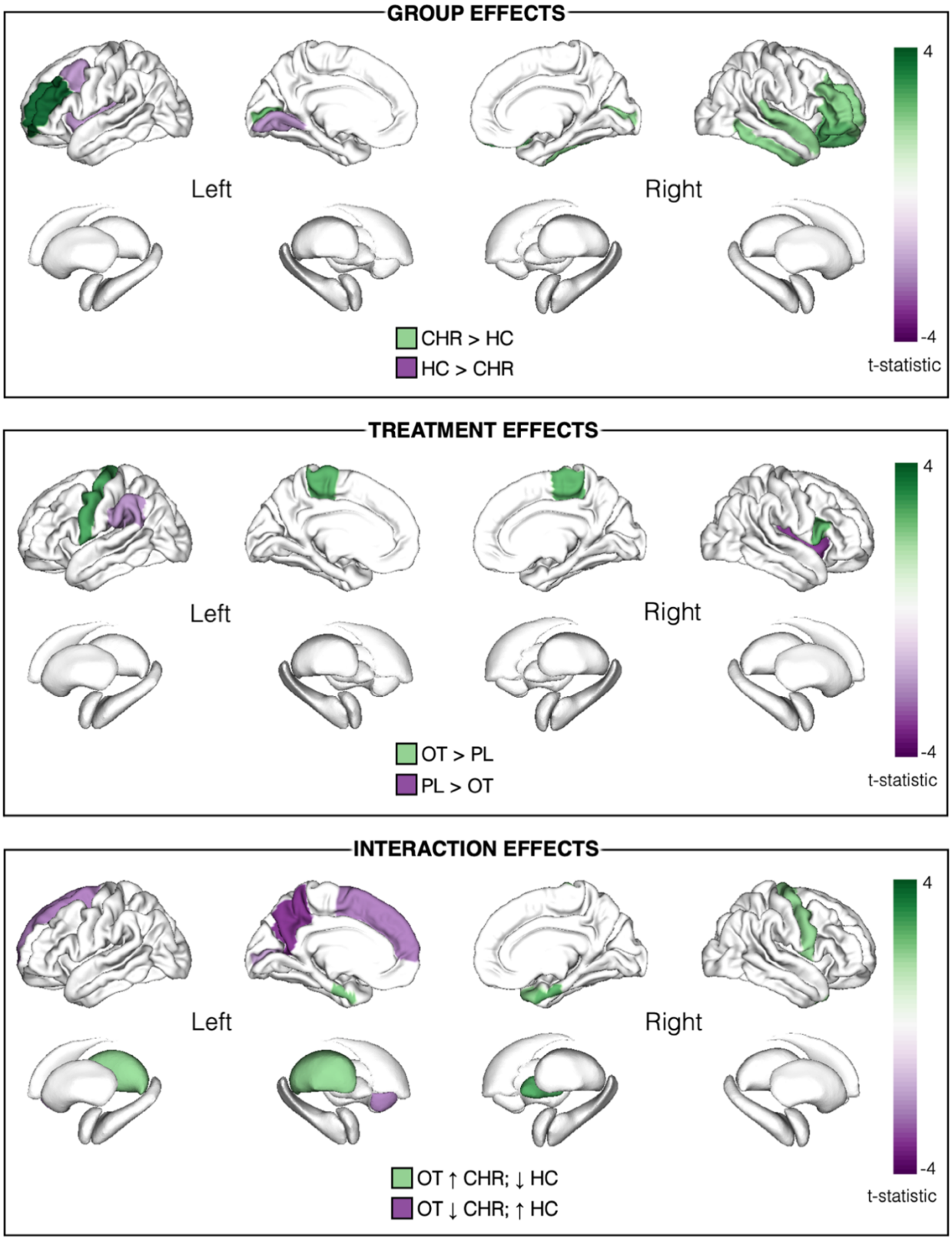


*Legend:* The shade of colour represents the t-statistic for each region. Only regions surviving FDR-corrected significance threshold p<.05 shown. In the top panel depicting main effects of group, regions in purple and green depict lower and greater graph metrics (respectively) in CHR-P relative to healthy controls (HC). In the middle panel depicting treatment effects, regions in green and purple depict increases and decreases (respectively) in graph metrics under oxytocin (OT) relative to placebo (PL). Although significant, the brainstem (t= 2.34) is not depicted as it is not included in

the ENIGMA visualisation template. In the lower panel depicting group x treatment interaction effects, regions in green depict where oxytocin increased (↑) graph metrics in the CHR-P group but decreased (↓) them in healthy controls; regions in purple depict where oxytocin decreased graph metrics in the CHR-P group but increased them in controls. All results are presented here irrespective of the metric; where there were effects in the same region in more than one nodal metric, the larger t-value is shown. All corresponding statistics are presented in Table 2 and individual figures for each metric are appended in Supplementary Figures 2-4.

**FIGURE 3.** Overlap between the group, treatment and interaction findings and the large-scale canonical resting-state networks (RSNs).

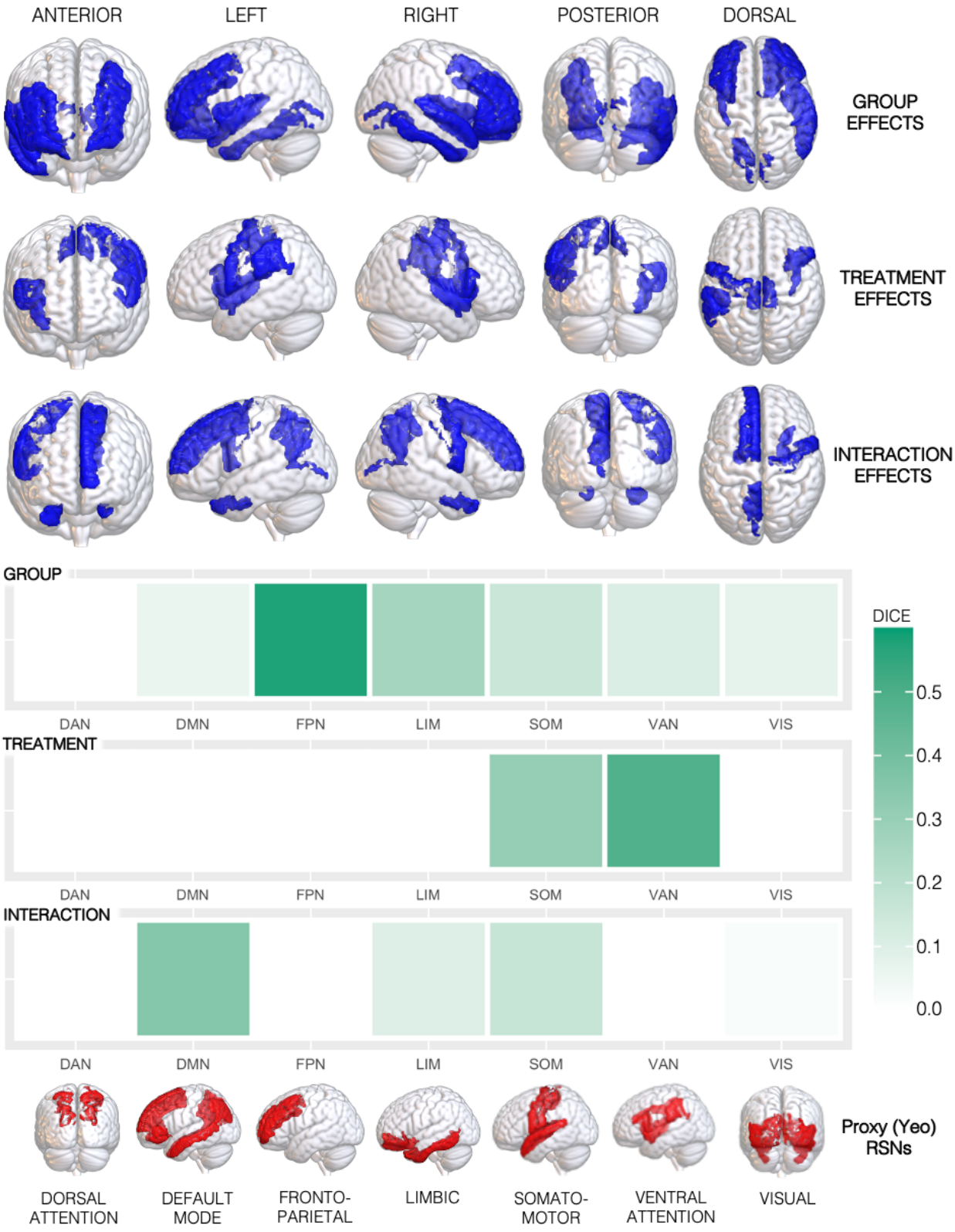


*Legend:* We calculated the percentage of overlap between our result maps—which included binary masks of all cortical regions showing differences in nodal metrics (for group, treatment and interaction effects, separately)—and the large-scale RSNs described in the atlas from Yeo et al. (65). As subcortical structures are not covered by the Yeo atlas, these were omitted from our result

maps to prevent artificial reduction of the overlap estimate. The Yeo atlas includes a coarse parcellation of 7 canonical RSNs: the default-mode (DMN), dorsal attention (DAN), frontoparietal (FPN), limbic (LIM), somatomotor (SOM), visual (VIS) and ventral attention (VAN) networks. We created a proxy DKA>Yeo atlas for each of the 7 Yeo RSNs by combining individual DKA regions, allocating each to a single RSN based on the RSN for which each region had the highest number of overlapping vertices based on the confusion matrix from a previous study (100). Overlap was quantified using the Dice-kappa coefficient, which measures the percentage of voxels of each RSN overlapping with our group/treatment/interaction effect maps. In the upper section, we provide an overview of all regions where we found group, treatment or interaction effects, irrespective of the specific graph metric, rendered in a 3D glass brain (semi-transparent) surface model. In the lower section, we provide a heatmap summarising the percentage of overlap (Dice-kappa coefficient) between our results and each of the 7 networks, with each network rendered in a 3D glass brain (semi-transparent) surface model. Note that despite the visualisation, regions belonging to the different RSNs do not overlap, for example, the FPN contains the rostral and caudal middle frontal gyri, wheras the DMN contains the superior and inferior frontal gyri, which are difficult to differentiate in rendered models.